Desmosine Content and Passive Mechanics of the Elastic Fiber Deficient Murine Uterus

Jasmine Kiley
Tulane University, New Orleans, Louisiana, USA

Abstract

Elastic fibers in the extracellular matrix provide compliance and distensibility to soft biological tissues, such as the uterus. The uterus grows and remodels during processes such as gestation and menstruation. Preterm birth may be associated with uterine overdistention, which can be exacerbated in females with underdeveloped elastic fibers. Desmosine crosslinks form between mature elastic fibers and can be used to infer the mature fiber content. Fibulin-5 (*Fbln5*) is expressed in tissues abundant in elastic fibers, and mice deficient in *Fbln5* develop pelvic floor disorders similar to females with genetic disorders that negatively impact elastic fiber formation. Prior work has quantified desmosine content to study elastic fiber turnover in the vagina of *Fbln5* deficient mice. However, the presence of mature elastic fibers in uterine tissue with varying *Fbln5* expression is unknown. Further, the influence of desmosine content on passive uterine mechanics is unknown. Therefore, the objective of this study was to determine the role of *Fbln5* insufficiency on desmosine content and its effect on passive mechanics of the murine uterus. We hypothesize that *Fbln5* haploinsufficient and deficient murine uterine tissue will have lower desmosine content than wildtype tissue. It is further hypothesized that *Fbln5* haploinsufficiency or deficiency will decrease the passive compliance and distensibility of the murine uterus. Characterizing the desmosine content and passive distensibility of the murine uterus may provide insight into the influence of elastic fiber deficiency on uterine function, which can be applied to the clinical setting to assess the etiology of pelvic floor disorders in women with disrupted elastic fiber development.

Introduction

The female reproductive system is comprised of the vagina, cervix, uterus, fallopian tubes, and ovaries. The uterus plays a critical role in gestation and menstruation, and one of its main functions is the ability to expand and remodel to accommodate these processes (Myers & Elad, 2017). There is a limit to the extent that the uterus can stretch in healthy pregnancies, and uterine overdistention is thought to lead to preterm labor in women carrying more than one fetus (Adams Waldorf et al., 2015). The incidence of preterm birth varies around the world, ranging from 3.6% in Germany to 14.7% in Egypt, and 35.8% of infant deaths are related to complications from preterm birth (Callaghan et al., 2006; Kiserud et al., 2017).

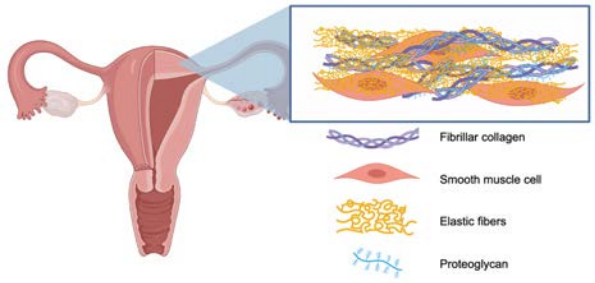

Figure 1. *Structure of the uterine extracellular matrix around smooth muscle cells, including fibrillar collagen, elastic fibers, and proteoglycan. Figure created with Biorender.com*

A key structural component of the extracellular matrix of uterine tissue that provides its compliance and distensibility are elastic fibers (Sherratt, 2009) (Leppert & Yu, 1991). For example, decreased elastic fiber integrity in vasculature results in decreased distensibility, or ability to radially expand (Ferruzzi et al., 2016). Genetic disorders such as Marfan syndrome negatively impact elastic fiber formation. Females with Marfan syndrome give birth significantly earlier than females without Marfan syndrome, and babies born to women with Marfan syndrome are significantly more likely to be small for gestational age (Curry et al., 2014). The physiological and mechanical causes of earlier birth dates and smaller size at birth are unknown, but deficiencies in elastic fiber formation in the uterus may contribute.

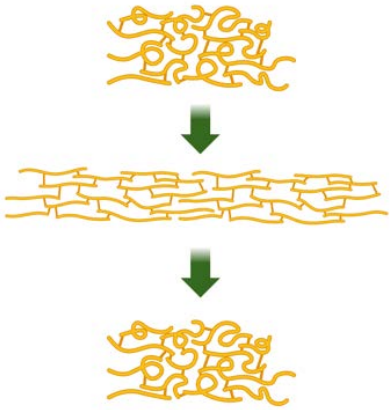

Figure 2. *Elastic fibers permit tissue to stretch and return (Akintunde et al., 2019) (Matthews et al., 2014). Figure created in biorender.com.*

Multiple proteins, such as fibulin-5 (*Fbln5*), are responsible for proper elastic fiber formation by binding elastin to a microfibril core. Further, elastin contains hydrophobic amino acids such as desmosine and intermolecular cross-links which are highly resistant to proteolytic degradation (Daamen et al., 2003). Desmosine is an indicator of elastic fiber maturity, and thus its quantity can be used to infer the amount of mature elastic fibers present in uterine tissue (Kielty et al., 2002).

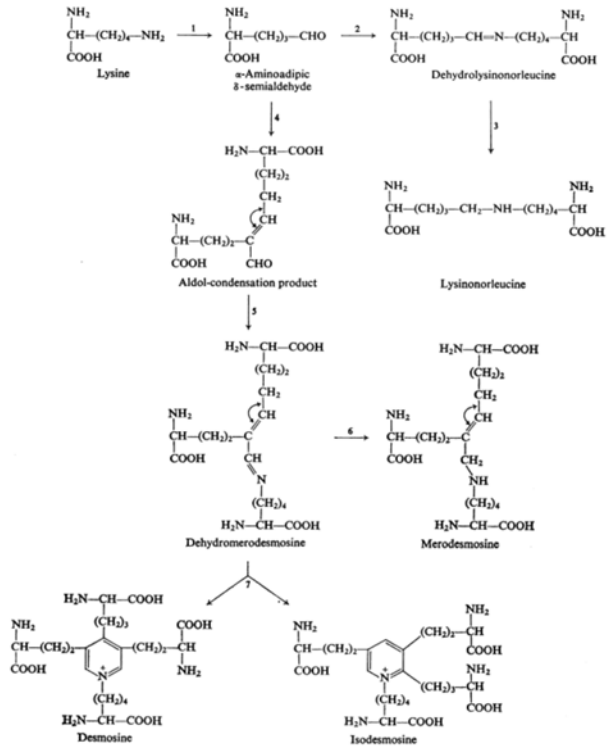

Figure 3. *The biosynthesis of desmosine from lysine residues (Francis et al., 1973).*

The biosynthesis of desmosine involves three lysine residues, beginning with oxidative deamination of the ε-amino

groups of two lysine residues into two molecules of α-aminoadipic δ-semialdehyde, also known as allysine (Francis et al., 1973). The two allysine molecules undergo an aldol condensation. Then, the aldol condensation product reacts with a third lysine residue via a Schiff-base formation to form dehydromerodesmosine, which goes on to form desmosine via a series of reactions that is not yet defined. Desmosine is formed alongside tropoelastin, the precursor to mature elastin (Gallop et al., 1972). Tropoelastin contains a large number of lysine side chains, which allow it to eventually form mature elastin crosslinked by desmosine in areas of high alanine content, as the small side chain allows space for the presence of these large crosslinks. This process is catalyzed by lysyl oxidase, which is the cross-linking enzyme of elastin and collagen (Halme et al., 1986).

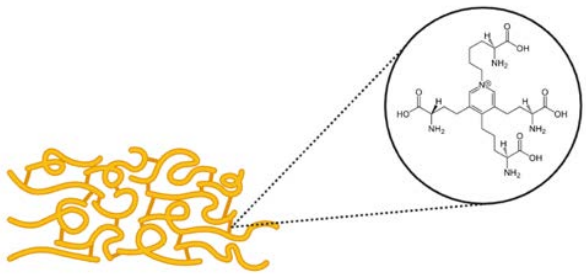

Figure 4. *Desmosine is found in crosslinks between mature elastic fibers (Daamen et al., 2003). Portions of the figure created in Biorender.com.*

Fbln5 is commonly expressed in tissues that contain an abundance of elastic fibers, including large blood vessels and the uterus. (Kowal et al., 1999). Mice that are deficient in *Fbln5* develop pelvic floor disorders similar to females with genetic disorders such as Marfan syndrome (Carley & Schaffer, 2000) (Drewes et al., 2007). *Fbln5* global knockout mice have been used to model vascular and pelvic organ pathologies (Clark-Patterson et al., 2021; Ramachandra et al., 2022). Through investigation of vaginal desmosine content as it relates to changes in elastic fiber homeostasis of *Fbln5* deficient mice, it has been shown that elastic fiber assembly after vaginal delivery is critical for reestablishment of pelvic organ support. (Drewes et al., 2007). However, the presence of mature elastic fibers in uterine tissue with differing expression of *Fbln5* is unknown. A need exists to quantify the amount of desmosine present in the uterine tissue of mice sufficient, haploinsufficient, and deficient in *Fbln5* to set a framework for conducting future investigations to determine how mature elastic fibers may impact the mechanical properties of the tissue. Further, the impact of *Fbln5* insufficiency on the ability of the uterus to expand is unknown.

Therefore, the objective of this study was to utilize the *Fbln5* knockout mouse model to determine the relationship between *Fbln5* genotype and desmosine content and its effect on passive distensibility of the murine uterus. Our specific aims were:

Aim 1: Quantify the desmosine content of *Fbln5* wildtype, haploinsufficient, and deficient murine uterine tissue. We hypothesize that *Fbln5* haploinsufficiency or deficiency will contribute to decreased desmosine content in comparison to wildtype controls.

Aim 2: Evaluate the passive mechanics in relation to the desmosine content of the murine uterus. We will use outer diameter measurements to calculate the normalized outer diameter and passive compliance of the tissue without smooth muscle contraction when pressurized with air. We hypothesize that *Fbln5* deficiency

will decrease the passive compliance and distensibility of the murine uterus compared to the wildtype and haploinsufficient uterus.

Aim 3: Evaluate methods improvement for determining the passive mechanics of the murine uterus. We will suggest alterations to the procedure implemented in this study to increase the efficacy of measurement and calculation of the passive mechanics of the murine uterus.

We expect to identify a relationship between desmosine content and passive distensibility to elucidate the contribution of mature elastic fibers to the passive mechanical properties of uterine tissue. This study may provide insight into the reproductive health and etiology of preterm birth in females with diseases that impact elastic fiber formation.

Methods

Animal Care

All procedures in this study received approval by the Institute Animal Care and Use Committee at Tulane University. This study performed all procedures in accordance with the relevant guidelines and regulations. The fibulin-5 *(Fbln5)* global knockout mice were developed by Dr. Hiromi Yanagisawa (Yanagisawa et al., 2002). The *Fbln5* colony was established at Tulane University from male and female breeders supplied by Dr. Jay Humphrey from Yale University. Female and male *Fbln5* haploinsufficient mice on mixed background (C57BL/6 × 129SvEv) generated all female wildtype ($Fbln5^{+/+}$,WT), haploinsufficient ($Fbln5^{+/-}$, HET), and deficient ($Fbln5^{-/-}$, KO) mice for use within this study. Microisolators housed all mice with littermates (no more than 5 per cage) under standard conditions with 12-h light and dark cycles. All mice were genotyped by tail snips taken during weaning by a commercial vendor (Transnetyx, Cordova, TN, USA) using real time PCR. An n = 18 female, nulliparous mice (6/genotype) were used in this study. All mice in this study were in the age range of 4-6 months, which correlates to approximately 28-35 years of age in humans (Dutta & Sengupta, 2016). Mice were euthanized with carbon dioxide and immediately dissected to extract the thoracic aorta, vagina, and uterus.

Dissection

A vertical cut using dissection scissors was made from the pubis to the top of the sternum. An I-cut was made to expose the abdominal cavity, and scissors were used to divide the rib cage and expose the pleural cavity. Using blunt forceps, the lungs were moved aside to expose the thoracic aorta. The thoracic aorta was separated from the spine using tweezers and blunt forceps, and then excised with microscissors. The aorta was maintained in 4 ˚C Hank's Balanced Saline Solution (HBSS) until dissection and mechanical testing were complete. In the abdominal cavity, the intestines were moved toward the sternum, and the visceral fat around the uterus was gently snipped away using microscissors. The left and right uterine horns were excised by a singular cut each at the proximal and distal ends of the horns to separate them from the cervix and ovaries, respectively. Each extracted organ was dried and weighed, then placed into 4 ˚C HBSS. One uterine horn was randomly allocated to undergo mechanical testing prior to storage for biomechanical testing.

Following mechanical testing, all samples were flash frozen and stored at -80 °C. The left and right uterine horns were stored separately.

Mechanical Testing

To evaluate the distensibility of the murine uterus, the outer diameter of the tissue was measured at 10 mmHg increments from 0-70 mmHg, which are within the physiologic range of uterine pressures (Humphrey, 2013; Milsom et al., 1988). A 10-millimeter segment of tissue was removed from the proximal side of the uterine horn. The intact cylindrical tissue was cannulated onto an extension-inflation device using two silk 6-0 sutures on each side (Figure X).

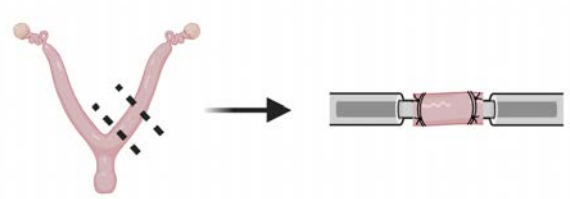

Figure 5. *Dissection and cannulation of uterine tissue in preparation for mechanical testing. Figure created in Biorender.com.*

The tissue was suspended in a bath of 4 °C HBSS. A sphygmomanometer was attached to one cannula, and the other cannula was pinched off to prevent airflow and pressure leakage. Each sample was pressurized up to approximately 75 mmHg and then released five times consecutively (Amin et al., 2012). Outer diameter measurements were taken in 10 mmHg increments for the third, fourth, and fifth pressurization cycles. Measurements were completed by measuring overhead images of the tissue using ImageJ (NIH, Bethesda, MD).

Biochemical Testing

To evaluate the concentration of desmosine in the uterine tissue, quantitative sandwich enzyme-linked immunosorbent assays (ELISAs) were conducted (Lifeome Biolabs, Oceanside, CA). This desmosine ELISA has high specificity and sensitivity for detection of murine desmosine and has been used in prior studies to quantify lung desmosine content (Seddon et al., 2013; Sellami et al., 2016). The thoracic aorta and vagina served as the positive control, as it has been previously noted that there is desmosine present in these organs (Drewes et al., 2007; Muto et al., 2013). To prepare for ELISA, the tissue samples were homogenized in 1 mL 1X phosphate buffered saline and then subjected to two freeze-thaw cycles. The ELISAs were then conducted as indicated by the kit to quantify the concentration of desmosine in the thoracic aorta, vagina, and left and right uterine horns.

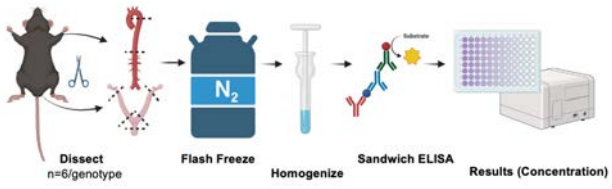

Figure 6. *Process of sample preparation and quantification of desmosine content via sandwich ELISA. Figure created in Biorender.com.*

Statistical Analysis

The sample size of n=6 for WT, HET, KO genotypes is similar to sample sizes used in prior studies involving sandwich ELISAs with mice (Lim et al., 2015; Shirakawa et al., 2022). Desmosine concentrations were analyzed with the Scheirer-Ray-Hare (SRH) test, followed by

Dunn's test with Benjamini-Hochberg corrections. The outer diameter measurements were used to calculate normalized outer diameter from 0 mmHg (Equation 1), stepwise compliance (Equation 2), and compliance from 0 mmHg (Equation 2). Normalized outer diameter was calculated using the following equation:

$$Normalized\ Diameter = \frac{D(P_n)}{D(P_0)}\ (Equation\ 1)$$

Where $D(P_n)$ is the outer diameter of the uterus at a given internal pressure and $D(P_0)$ is the diameter at and internal pressure of 0 mmHg.

Compliance was calculated using the following equation:

$$C(P) = \frac{\Delta A(P)}{\Delta P} \qquad (Equation\ 2)$$

Where $\Delta A(P)$ is the change in the luminal area at an intraluminal pressure P. The inner area was computed with inner radius, which was calculated as outer radius minus the thickness of the tissue (Naito et al., 2014). The thickness of tissue was noted as 0.61 mm for WT and 0.56 mm for KO, based on measurements of 4 month old and 11 month old WT mice, respectively. The 11 month thickness was used for the KO samples because the Fib5 KO has been described as a model of aging due to the disruption in elastic fibers (Hare et al., 2021).

Each mechanical property was analyzed with the Lilliefors test for normality and Levene's Test for equal variance, followed by a mixed ANOVA and Tukey's post hoc test if data was significant. The Pearson correlation coefficient and t-test for correlation was used to determine any correlation between biochemical and biomechanical data sets.

Results

Desmosine Content

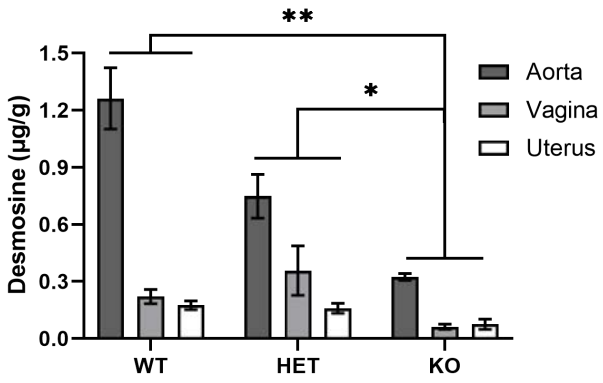

Figure 7. *Desmosine concentration in the Fbln5 WT, HET, and KO mice (n=6/group) in the aorta (dark grey), uterus (light grey), and vagina (white). Desmosine concentration was significantly lower in all KO organs (uterus, vagina, aorta) than HET (p=0.013) and WT organs (p=0.010). No significant interactions were identified between groups.*

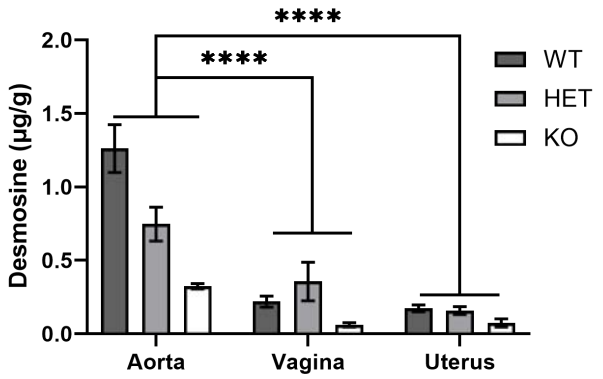

Figure 8. *Desmosine concentration in the aorta, uterus, and vagina with Fbln5 WT (dark grey), HET (light grey), and KO (white) (n=6/group). Desmosine concentration was significantly*

higher in aorta than uterus (p<0.001) and vagina (p<0.001) across all genotypes. No significant interactions were identified between groups.

An SRH test (genotype, organ) identified significant differences in desmosine content between genotypes (p=0.007) and organs (p<0.001), with no significant interactions. Desmosine content in all KO organs was significantly lower than HET (p=0.013) and WT organs (p=0.010) (Figure X). Desmosine content was higher in aorta compared to uterus (p<0.001) and vagina (p<0.001) across all genotypes (Figure X).

Normalized Outer Diameter

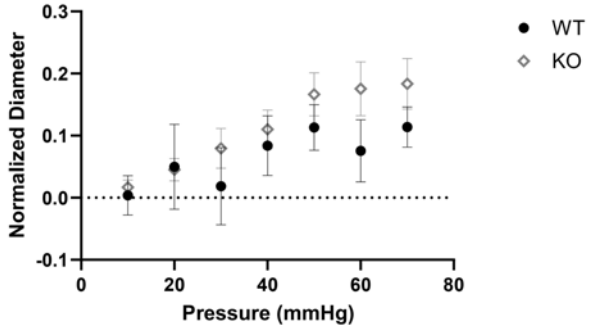

Figure 9. *Normalized uterine outer diameter of Fbln5 WT (circle) and KO (diamond) mice (n=4/group). A mixed ANOVA (genotype, pressure) followed by Tukey's post hoc tests showed a significant difference in normalized outer diameter between 10 mmHg and 70 mmHg (p=0.034). No significant interactions were identified between groups.*

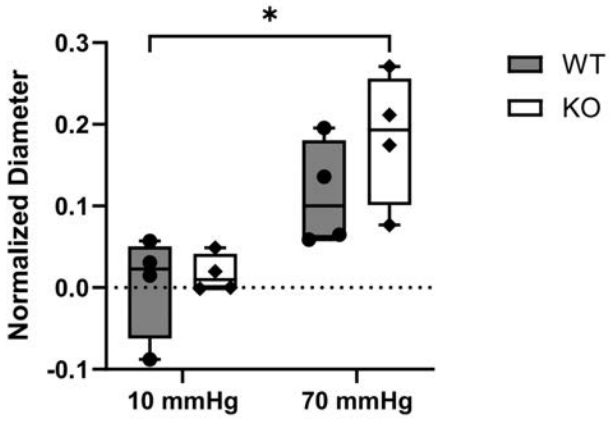

Figure 10. *Normalized uterine outer diameter of Fbln5 WT (grey) and KO (white) mice (n=4/group) at 10 mmHg internal pressure and 70 mmHg internal pressure. A mixed ANOVA (genotype, pressure) followed by Tukey's post hoc tests showed a significant difference in normalized outer diameter between 10 mmHg in the KO samples and 70 mmHg in the WT samples (p=0.034). No significant interactions were identified between groups.*

Calculations of normalized diameter followed by a mixed ANOVA (genotype, pressure) showed that the WT uterus at 70 mmHg of internal pressure had a significantly larger normalized outer diameter than the KO uterus at 10 mmHg.

Compliance

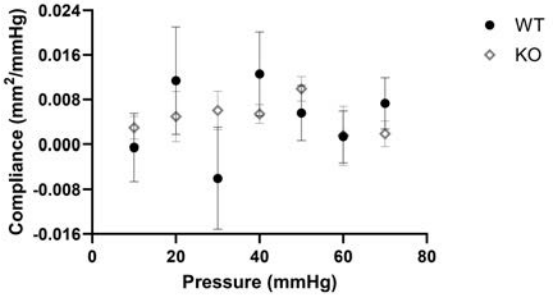

Figure 11. *Stepwise compliance in uterine tissue of Fbln5 WT (circle) and KO (diamond) mice (n=4/group). A mixed ANOVA did not indicate any significant differences in genotype or pressure.*

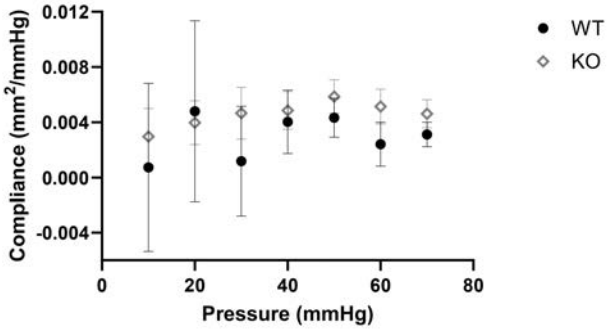

Figure 12. *Uterine compliance measured compared to 0 mmHg of Fbln5 WT (circle) and KO (diamond) mice (n=4/group). A mixed ANOVA did not indicate any significant differences in genotype or pressure.*

A mixed ANOVA did not indicate any significant differences in genotype or pressure for stepwise uterine compliance or overall uterine compliance (compared to 0 mmHg internal pressure).

Pearson Correlation Coefficient

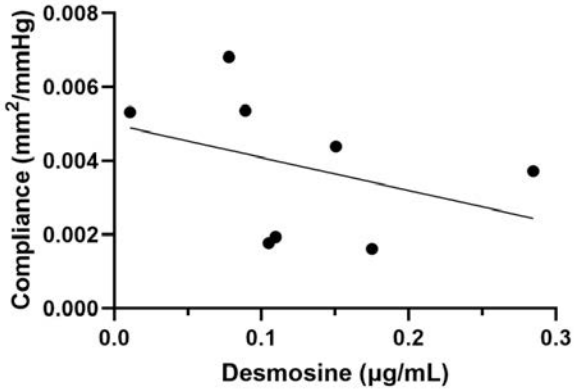

Figure 13. *Correlation between desmosine content and overall compliance measured at 70 mmHg of the murine uterus. A t-test indicated no significant correlation between desmosine content and overall compliance (p=0.18). The Pearson correlation coefficient was R=-0.3715, indicating a weak negative correlation between the two variables. The coefficient of determination was R^2=0.138. This indicates that 13.8% of the overall compliance can be predicted by desmosine content.*

Analysis with a Pearson correlation coefficient showed a weak negative correlation between desmosine content and overall compliance of uterine tissue when pressurized at 70 mmHg compared to 0 mmHg of internal pressure.

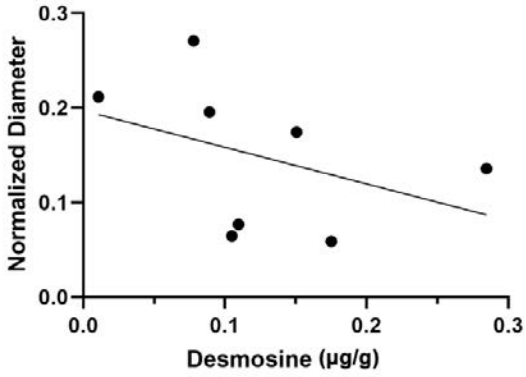

Figure 14. *Correlation between desmosine content and normalized murine uterine outer diameter. A t-test indicated no significant correlation between desmosine content and normalized outer diameter (p=0.16).The Pearson correlation coefficient was R=-0.4031, indicating a moderate negative correlation between the two variables. The coefficient of determination was R^2=0.1625. This indicates that 16.25% of the normalized outer diameter can be predicted by desmosine content.*

Analysis with a Pearson correlation showed a moderate negative correlation between desmosine content and normalized outer diameter.

Discussion

This investigation sought to elucidate the impacts of fibulin-5 haploinsufficiency and deficiency on the desmosine content and passive mechanics of murine uterine tissue. Desmosine concentration was significantly lower in the KO organs than other genotypes, indicating that the KO *Fbln5* genotype leads to lower levels of desmosine in the uterus than in the HET and WT mouse. This aligns with the changes in desmosine content of the murine vagina with *Fbln5* haploinsufficiency and deficiency as noted in prior work (Drewes et al., 2007). This may provide insight into the presence of mature elastic fibers in uterine tissue to advance a fundamental understanding of the uterine composition which could improve our understanding of the etiology of preterm birth in females with genetic disorders that lead to underdeveloped elastic fibers.

Normalized outer diameter in the KO uterus at 10 mmHg was significantly smaller than the WT uterus at 70 mmHg of internal pressure. However, at 70 mmHg of internal pressure the WT uterus does not expand enough to have a significantly larger normalized outer diameter than the WT uterus at other lower internal pressures. Additionally, the normalized outer diameter at 70 mmHg between the WT and KO genotypes does not show a significant difference. This indicates that, despite decreased desmosine content, the KO uterus expands in a comparable manner to the WT uterus at 70 mmHg, although neither genotype expands enough to be significantly different than the normalized outer diameter of the same genotype at lower internal pressures. It is possible that there are additional aspects of the tissue that compensate for the elasticity lost by underdeveloped elastic fibers in the KO samples. Some of these may include other elastin crosslinking proteins such as fibulin-4 and fibulin-3 (Horiguchi et al., 2009; Rahn et al., 2009).

There was a moderate negative correlation detected between desmosine content and normalized outer diameter and a weak negative correlation detected between desmosine content and overall compliance of the murine uterus. This indicates that increased desmosine content contributes to lower distensibility and compliance of the tissue. While desmosine content does play a role in passive uterine mechanics, the lack of stronger correlation is most likely due to other factors that influence the normalized outer diameter and compliance of murine uterine tissue beyond desmosine content, such as fibulin-4 and fibulin-3 or other matrix components such as collagen, which provides tensile strength to the tissue (Kerkhof et al., 2009; Rahn et al., 2009).

Limitations and Methods Improvement

Desmosine content previously reported in the aorta and vagina were taken in comparison to the dry weight of the organ, while this study utilized fresh weight, so the levels cannot be directly compared. Future iterations of this study could incorporate desiccation of the tissue samples prior to recording the mass and conducting biochemical testing.

The original sample size for mechanical testing was n=6/genotype, but two WT and KO samples each and four HET samples were excluded. The exclusion was due to St. Venant's principle, which requires that the length of the tissue sample between cannulas must exceed the outer diameter in order for the measurements of diameter change to be valid. The two

remaining HET samples were not included in statistical analysis because of the lack of standard deviation. In future experiments, the uterine tissue will be cut to a length of 15 mm in order to provide a greater margin for securing the tissue sample onto the cannula using sutures. Additionally, there were some instances in which the uterine tissue burst during pressurization due to weakness of the uterine wall. It is important to preserve a second section of the uterine horn in order to have a backup sample of tissue in its native cylindrical shape if the original section of tissue does not withstand five cycles of pressurization.

The camera used to record the pressurization of the murine uterus was an iPhone XR, and it was noted that the maximum change in outer diameter was only a difference of a few pixels in ImageJ. In future experiments, a higher resolution camera should be used for recordings in order to capture the change in outer diameter in greater sensitivity.

Conclusion and Future Directions

This study demonstrated that the KO *Fbln5* genotype led to decreased levels of desmosine in murine uterine tissue. It was also shown that the normalized outer diameter of the WT uterus at 70 mmHg internal pressure is significantly wider than the normalized outer diameter of the KO uterus at 10 mmHg internal pressure. This work may provide insight as to the passive uterine mechanics and uterine mature elastic fiber composition of women with diseases associated with underdeveloped elastic fibers. It remains unknown whether the KO uterus sustains similar microstructural changes as the WT uterus when experiencing mechanical loading from internal pressure. Future steps include analysis of the microstructure of the uterine tissue during gestation and postpartum healing to understand potential differences in microstructural changes due to increased internal pressure.

Acknowledgments

I would like to thank Dr. Kristin S. Miller for her mentorship over the course of my undergraduate research experience and for allowing me to partake in this project funded by the NSF Early Faculty CAREER Development Award (CMMI-1751050 (KSM)). Dr. Miller's guidance and support has been integral to my trajectory as an aspiring physician who seeks to practice in academic medicine, and her expertise in biomechanics was incredibly helpful over the course of this work.

I would also like to thank Dr. Robert Pascal for his guidance in the biochemical aspects of this project. His courses allowed my love of biochemistry to flourish, and his lively teaching style has inspired the educator that I hope to become. Additionally, I would like to thank Dr. Brittany Kennedy for her guidance as to the interdisciplinary aspects of this project. Her support in and out of the classroom has pushed me to become a well-rounded future physician who is equipped to serve diverse patient populations.

I would also like to thank Mari Domingo for her support in figure assembly, Qinhan Zhou for his patience and guidance as I learned to use R for statistical analysis, and Dr. Shelby White for her support throughout the data collection and writing phases of this project.

Along with the NSF grant, this work was supported by the Newcomb Tulane College Grant, the Stamps Scholarship, and

the Tulane University Office of Academic Enrichment summer research award.

References

Adams Waldorf, K. M., Singh, N., Mohan, A. R., Young, R. C., Ngo, L., Das, A., Tsai, J., Bansal, A., Paolella, L., Herbert, B. R., Sooranna, S. R., Gough, G. M., Astley, C., Vogel, K., Baldessari, A. E., Bammler, T. K., MacDonald, J., Gravett, M. G., Rajagopal, L., & Johnson, M. R. (2015). Uterine overdistention induces preterm labor mediated by inflammation: observations in pregnant women and nonhuman primates. *Am J Obstet Gynecol*, *213*(6), 830.e831-830.e819. https://doi.org/10.1016/j.ajog.2015.08.028

Akintunde, A. R., Robison, K. M., Capone, D. J., Desrosiers, L., Knoepp, L. R., & Miller, K. S. (2019). Effects of Elastase Digestion on the Murine Vaginal Wall Biaxial Mechanical Response. *J Biomech Eng*, *141*(2), 0210111-02101111. https://doi.org/10.1115/1.4042014

Amin, M., Le, V. P., & Wagenseil, J. E. (2012). Mechanical testing of mouse carotid arteries: from newborn to adult. *J Vis Exp*(60). https://doi.org/10.3791/3733

Callaghan, W. M., MacDorman, M. F., Rasmussen, S. A., Qin, C., & Lackritz, E. M. (2006). The contribution of preterm birth to infant mortality rates in the United States. *Pediatrics*, *118*(4), 1566-1573. https://doi.org/10.1542/peds.2006-0860

Carley, M. E., & Schaffer, J. (2000). Urinary incontinence and pelvic organ prolapse in women with Marfan or Ehlers Danlos syndrome. *Am J Obstet Gynecol*, *182*(5), 1021-1023. https://doi.org/10.1067/mob.2000.105410

Clark-Patterson, G. L., Roy, S., Desrosiers, L., Knoepp, L. R., Sen, A., & Miller, K. S. (2021). Role of fibulin-5 insufficiency and prolapse progression on murine vaginal biomechanical function. *Scientific Reports*, *11*(1), 20956. https://doi.org/10.1038/s41598-021-00351-1

Curry, R. A., Gelson, E., Swan, L., Dob, D., Babu-Narayan, S. V., Gatzoulis, M. A., Steer, P. J., & Johnson, M. R. (2014). Marfan syndrome and pregnancy: maternal and neonatal outcomes. *Bjog*, *121*(5), 610-617. https://doi.org/10.1111/1471-0528.12515

Daamen, W. F., van Moerkerk, H. T., Hafmans, T., Buttafoco, L., Poot, A. A., Veerkamp, J. H., & van Kuppevelt, T. H. (2003). Preparation and evaluation of molecularly-defined collagen-elastin-glycosaminoglycan scaffolds for tissue engineering. *Biomaterials*, *24*(22), 4001-4009. https://doi.org/10.1016/s0142-9612(03)00273-4

Drewes, P. G., Yanagisawa, H., Starcher, B., Hornstra, I., Csiszar, K., Marinis, S. I., Keller, P., & Word, R. A. (2007). Pelvic organ prolapse in fibulin-5 knockout mice: pregnancy-induced changes in elastic fiber homeostasis in mouse vagina. *Am J Pathol*, *170*(2), 578-589. https://doi.org/10.2353/ajpath.2007.060662

Dutta, S., & Sengupta, P. (2016). Men and mice: Relating their ages. *Life Sci*,

152, 244-248. https://doi.org/10.1016/j.lfs.2015.10.025

Ferruzzi, J., Bersi, M. R., Mecham, R. P., Ramirez, F., Yanagisawa, H., Tellides, G., & Humphrey, J. D. (2016). Loss of Elastic Fiber Integrity Compromises Common Carotid Artery Function: Implications for Vascular Aging. *Artery Res*, *14*, 41-52. https://doi.org/10.1016/j.artres.2016.04.001

Francis, G., John, R., & Thomas, J. (1973). Biosynthetic pathway of desmosines in elastin. *Biochem J*, *136*(1), 45-55. https://doi.org/10.1042/bj1360045

Gallop, P. M., Blumenfeld, O. O., & Seifter, S. (1972). Structure and metabolism of connective 801 tissue proteins. *Annu Rev Biochem*, *41*, 617-672. https://doi.org/10.1146/annurev.bi.41.070172.003153

Halme, T., Vihersaari, T., & Penttinen, R. (1986). Lysyl oxidase activity and synthesis of desmosines in cultured human aortic cells and skin fibroblasts: comparison of cell lines from control subjects and patients with the Marfan syndrome or other annulo-aortic ectasia. *Scand J Clin Lab Invest*, *46*(1), 31-37. https://doi.org/10.3109/00365518609086478

Hare, A. M., Gaddam, N. G., Shi, H., Acevedo, J. F., Word, R. A., & Florian-Rodriguez, M. E. (2021). Impact of vaginal distention on cell senescence in an animal model of pelvic organ prolapse. *Tissue Cell*, *73*, 101652. https://doi.org/10.1016/j.tice.2021.101652

Horiguchi, M., Inoue, T., Ohbayashi, T., Hirai, M., Noda, K., Marmorstein, L. Y., Yabe, D., Takagi, K., Akama, T. O., Kita, T., Kimura, T., & Nakamura, T. (2009). Fibulin-4 conducts proper elastogenesis via interaction with cross-linking enzyme lysyl oxidase. *Proceedings of the National Academy of Sciences of the United States of America*, *106*(45), 19029-19034. https://doi.org/10.1073/pnas.0908268106

Humphrey, J. D. (2013). *Cardiovascular solid mechanics: cells, tissues, and organs*. Springer Science & Business Media.

Kerkhof, M. H., Hendriks, L., & Brölmann, H. A. (2009). Changes in connective tissue in patients with pelvic organ prolapse--a review of the current literature. *Int Urogynecol J Pelvic Floor Dysfunct*, *20*(4), 461-474. https://doi.org/10.1007/s00192-008-0737-1

Kielty, C. M., Sherratt, M. J., & Shuttleworth, C. A. (2002). Elastic fibres. *J Cell Sci*, *115*(Pt 14), 2817-2828. https://doi.org/10.1242/jcs.115.14.2817

Kiserud, T., Piaggio, G., Carroli, G., Widmer, M., Carvalho, J., Neerup Jensen, L., Giordano, D., Cecatti, J. G., Abdel Aleem, H., Talegawkar, S. A., Benachi, A., Diemert, A., Tshefu Kitoto, A., Thinkhamrop, J., Lumbiganon, P., Tabor, A., Kriplani, A., Gonzalez Perez, R., Hecher, K., . . . Platt, L. D. (2017). The World Health Organization Fetal Growth Charts: A Multinational Longitudinal Study of Ultrasound Biometric Measurements and Estimated Fetal Weight. *PLoS Med*, *14*(1), e1002220.

https://doi.org/10.1371/journal.pmed.1002220

Kowal, R. C., Richardson, J. A., Miano, J. M., & Olson, E. N. (1999). EVEC, a novel epidermal growth factor-like repeat-containing protein upregulated in embryonic and diseased adult vasculature. *Circ Res*, *84*(10), 1166-1176. https://doi.org/10.1161/01.res.84.10.1166

Leppert, P. C., & Yu, S. Y. (1991). Three-dimensional structures of uterine elastic fibers: scanning electron microscopic studies. *Connect Tissue Res*, *27*(1), 15-31. https://doi.org/10.3109/03008209109006992

Lim, Y., Zhong, J. H., & Zhou, X. F. (2015). Development of mature BDNF-specific sandwich ELISA. *J Neurochem*, *134*(1), 75-85. https://doi.org/10.1111/jnc.13108

Matthews, A., Hutnik, C., Hill, K., Newson, T., Chan, T., & Campbell, G. (2014). Indentation and needle insertion properties of the human eye. *Eye (Lond)*, *28*(7), 880-887. https://doi.org/10.1038/eye.2014.99

Milsom, I., Andersch, B., & Sundell, G. (1988). The effect of flurbiprofen and naproxen sodium on intra-uterine pressure and menstrual pain in patients with primary dysmenorrhea. *Acta Obstet Gynecol Scand*, *67*(8), 711-716. https://doi.org/10.3109/00016349809004294

Muto, T., Miyajima, A., Bamba, M., & Hirota, T. (2013). Disruption of elastic lamellae in the aorta by D-penicillamine and its effect on vaso-regulation in rats. *J Toxicol Sci*, *38*(5), 707-717. https://doi.org/10.2131/jts.38.707

Myers, K. M., & Elad, D. (2017). Biomechanics of the human uterus. *Wiley Interdiscip Rev Syst Biol Med*, *9*(5). https://doi.org/10.1002/wsbm.1388

Naito, Y., Lee, Y. U., Yi, T., Church, S. N., Solomon, D., Humphrey, J. D., Shin'oka, T., & Breuer, C. K. (2014). Beyond burst pressure: initial evaluation of the natural history of the biaxial mechanical properties of tissue-engineered vascular grafts in the venous circulation using a murine model. *Tissue Eng Part A*, *20*(1-2), 346-355. https://doi.org/10.1089/ten.TEA.2012.0613

Rahn, D. D., Acevedo, J. F., Roshanravan, S., Keller, P. W., Davis, E. C., Marmorstein, L. Y., & Word, R. A. (2009). Failure of pelvic organ support in mice deficient in fibulin-3. *Am J Pathol*, *174*(1), 206-215. https://doi.org/10.2353/ajpath.2009.080212

Ramachandra, A. B., Mikush, N., Sauler, M., Humphrey, J. D., & Manning, E. P. (2022). Compromised Cardiopulmonary Function in Fibulin-5 Deficient Mice. *J Biomech Eng*, *144*(8). https://doi.org/10.1115/1.4053873

Seddon, J., Kasprowicz, V., Walker, N. F., Yuen, H. M., Sunpath, H., Tezera, L., Meintjes, G., Wilkinson, R. J., Bishai, W. R., Friedland, J. S., & Elkington, P. T. (2013). Procollagen III N-terminal propeptide and desmosine are released by matrix destruction in pulmonary tuberculosis. *J Infect Dis*, *208*(10), 1571-1579. https://doi.org/10.1093/infdis/jit343

Sellami, M., Meghraoui-Kheddar, A., Terryn, C., Fichel, C., Bouland, N.,

Diebold, M. D., Guenounou, M., Héry-Huynh, S., & Le Naour, R. (2016). Induction and regulation of murine emphysema by elastin peptides. *Am J Physiol Lung Cell Mol Physiol*, *310*(1), L8-23. https://doi.org/10.1152/ajplung.00068.2015

Sherratt, M. J. (2009). Tissue elasticity and the ageing elastic fibre. *Age (Dordr)*, *31*(4), 305-325. https://doi.org/10.1007/s11357-009-9103-6

Shirakawa, T., Ikushima, A., Maruyama, N., Nambu, Y., Awano, H., Osawa, K., Nirasawa, K., Negishi, Y., Nishio, H., Fukushima, S., & Matsuo, M. (2022). A sandwich ELISA kit reveals marked elevation of titin N-terminal fragment levels in the urine of mdx mice. *Animal Model Exp Med*, *5*(1), 48-55. https://doi.org/10.1002/ame2.12204

Yanagisawa, H., Davis, E. C., Starcher, B. C., Ouchi, T., Yanagisawa, M., Richardson, J. A., & Olson, E. N. (2002). Fibulin-5 is an elastin-binding protein essential for elastic fibre development in vivo. *Nature*, *415*(6868), 168-171. https://doi.org/10.1038/415168a